Journal of Chemistry and Technologies, 2024, *32*(4), 887-894

Journal of Chemistry and Technologies

pISSN 2663-2934 (Print), ISSN 2663-2942 (Online).

journal homepage: http://chemistry.dnu.dp.ua
editorial e-mail: chem.dnu@gmail.com

UDC 544.77 + 544.032.6

VISIBLE LIGHT ACTIVE FLUORITE-TYPE NANOCOMPOSITES FORMED IN THE CeO_2-La_2O_3-Dy_2O_3 SYSTEM

Olena M. Lavrynenko, Maksym M. Zahornyi*, Oksana A. Korniienko, Serhii F. Korichev, Alisa R. Atamanchuk

I. Frantsevich Institute for Problems of Materials Science, NAS of Ukraine, 3 Omeliana Pritsaka str., 03680 Kyiv, Ukraine

Received 8 September 2024; accepted 15 November 2024; available online 25 January 2025

Abstract

Fluorite-type nanocomposite materials with a content of 95–60 mol.% CeO_2, 10–20 mol.% La_2O_3, and 5–20 mol.% Dy_2O_3 were obtained by the chemical co-precipitation method using REE (rare earth elements) nitrate solutions. The primary particle size (coherent scattering region) increased from 11.3 to 26.5 nm when the calcination temperature increased from 600 to 800 °C. The highest photocatalytic activity in the destruction of Malachite green dye under the influence of visible light was shown by the sample with the composition of CeO_2 (80 mol.%) - La_2O_3 (10 mol.%) - Dy_2O_3 (10 mol.%), thermally treated at 600 °C for 5 hours. The results of the experimental study showed that at the initial concentration of the Malachite green (MG) solution of 20 mg/dm³ under the influence of visible light for 1 hour, its residual concentration was only 0.45 mg/dm³, and the degree of decolorization of the solution reached 98 %. It is assumed that nanocomposites based on a CeO_2-La_2O_3-Dy_2O_3 solid solution with a fluorite-type structure can be used to create effective photocatalysts designed for the destruction of cationic dyes in an aqueous medium.

Keywords: nanocomposite; CeO_2-La_2O_3-Dy_2O_3; fluorite-type structure; visible light photocatalytic activity; Malachite Green; dye destruction.

АКТИВНІ У ДІАПАЗОНІ ВИДИМОГО СВІТЛА НАНОКОМПОЗИТИ ЗІ СТРУКТУРОЮ ФЛЮОРИТУ, ОТРИМАНІ В СИСТЕМІ CeO_2-La_2O_3-Dy_2O_3

Олена М. Лавриненко, Максим М. Загорний, Оксана А. Корнієнко, Сергій Ф. Коричев, Аліса Р. Атаманчук

Інститут проблем матеріалознавства ім. І.М. Францевича НАН України, вул. Омеляна Пріцака 3, Київ, 03680, Україна

Анотація

Методом хімічного співосадження з використанням розчинів нітратів РЗЕ отримано зразки нанокомпозитних матеріалів зі структурою типу флюориту, які містили 95–60 мол.% CeO_2, 10–20 мол.% La_2O_3 та 5–20 мол.% Dy_2O_3. Розмір первинних частинок (область когерентного розсіювання) збільшувалась від 11,3 до 26,5 нм при підвищенні температури прожарювання з 600 до 800 °C. Найвищу фотокаталітичну активність у деструкції барвника малахітового зеленого під впливом видимого світла виявив зразок складу CeO_2 (80 мол.%) – La_2O_3 (10 мол.%) – Dy_2O_3 (10 мол.%), термічно оброблений при 600 °C протягом 5 годин. Результати дослідження показали, що при вихідній концентрації розчину малахітового зеленого 20 мг/дм³ під впливом видимого світла протягом 1 години його залишкова концентрація становила лише 0.45 мг/дм³, а ступінь знебарвлення розчину досягав 98 %. Передбачається, що нанокомпозити на основі твердого розчину CeO_2-La_2O_3-Dy_2O_3 зі структурою типу флюориту можуть бути використані для створення ефективних фотокаталізаторів, призначених для деструкції катіонних барвників у водному середовищі.

Ключові слова: нанокомпозит; CeO_2-La_2O_3-Dy_2O_3; структура типу флюориту; фотокаталітична активність у видимому світлі; малахітовий зелений; руйнування барвника.

**Corresponding author: e-mail: mzahornyi81@gmail.com*

doi: 10.15421/jchemtech.v32i4.311116

Journal of Chemistry and Technologies, 2024, *32*(4), 887-894

Introduction

Today, among all oxides of rare earth metals, nanostructured cerium dioxide (CeO_2) has become the most widely used in the creation of functional materials for technical purposes, in particular, catalysts, conductors, electrodes, luminescent and optical devices, sensors, etc. [1–4]. Nanoceria is recognized as a promising material for the creation of biomedical devices and drugs, methane oxidation, and energy storage applications [5–8]. Nanostructures based on cerium dioxide and rare earth elements are characterized by thermal and chemical stability, high ionic conductivity, their ability to accumulate or release oxygen, strong absorption of UV rays, etc. [8–11].

The high photocatalytic activity of cerium dioxide is based on the presence of Ce^{3+} /Ce^{4+} redox couple on the surface of the particles. It is known that when trivalent lanthanide ions replace Ce^{4+} ions in the structure of the composite, an increase in chemical stability and improvement of the ionic conductivity of the obtained material is expected [12]. For example, authors [13] showed that La^{3+} significantly increased the catalytic activity of CeO_2; the best results were obtained at 5 wt.% lanthanum. Therefore, solid solutions based on CeO_2 are promising for creating electrodes and electrolytes in solid oxide fuel (SOFC) and electrolysis (SOEC) cells.

The effect of metal admixture on the optical and photocatalytic properties of cerium dioxide nanoparticles was investigated in [14–16] and it was shown that doped lanthanum nanoparticles are of interest as chemically stable photoluminescent materials [15].

In recent years, scientific research has paid great attention to the development and improvement of methods for the synthesis of nanostructured cerium and lanthanum oxides [15; 16]. One of the reliable methods for the synthesis of mesoporous pure and mixed oxides of lanthanum and cerium is the microemulsion method [17], which allows obtaining nanostructures with a specific surface area ~110 m^2/g at 450 C. In work [18], CeO_2 nanocrystalline powders doped with La^{3+} ions were obtained using a modified sol-gel process.

Typically, dysprosium oxide is used as an alloying agent in the production of powerful permanent magnets, ceramics, luminescent materials and the doping of cerium dioxide with dysprosium led to an increase in ionic conductivity and lower activation energy of the nanocomposites compared to the undoped sample [19]. The results of the photoluminescence study of dysprosium-doped CeO_2 particles are discussed in [20]. The resulting composites are promising for application in displays and optical devices. In particular, doping CeO_2 nanoparticles with dysprosium oxide improved their chemical, optical, and fluorescent properties compared to undoped cerium dioxide [21].

It should be noted that there is currently growing interest in the development and implementation of materials obtained in ternary composite systems. For example, in work [22] the catalytic application of nanomaterials based on cerium oxide doped with lanthanum and dysprosium is considered in detail. The works [23–24] present the results of the research of synthesized nanopowders based on $Dy_2Ce_2O_7$ and investigate their photocatalytic properties under the UV irradiation.

In general, based on information about the structure of state diagrams of binary [25] and ternary systems [25–27] based on cerium dioxide doped with La ions, it can be stated that in a wide range of concentrations and temperatures, stable solid solutions with a fluorite-type structure are formed, which allow to vary the amount of alloying admixture and, as a result, to change the physical and chemical properties of the resulting composites. The authors [28] introduced lanthanum (La) and dysprosium (Dy) into the crystal structure of CeO_2 at the same time using sol-gel synthesis and chemical synthesis with the addition of citric acid. The sintering temperatures of the precipitates were set at 800 and 1000 °C. X-ray diffraction (XRD) results showed that doped and undoped CeO_2 compounds form a cubic phase. The particle sizes ranged from 90 to 150 nm. The photocatalytic behaviour of the compounds was studied using Methylene blue dye decomposition. The dye degradation efficiency for the $Ce_{0.85}La_{0.10}Dy_{0.05}O_2$ composition system was only 60 % in 100 min using a 300 W xenon lamp.

Our works present the results of synthesized nanosized cerium and lanthanum dioxide powders [29] with their structural characteristics and morphology. We study selectively optical, photocatalytic, and antibacterial properties, which determine the suitability of materials for biomedicine [29–31].

This work aims to obtain nanopowders of cerium dioxide and composites based on it, doped with lanthanum and dysprosium, study their structure and photocatalytic activity under visible light conditions.

Research objects and methods

The synthesis of composite particles was carried out by a chemical co-precipitation of the cerium, lanthanum, and dysprosium nitrate's solutions in the presence of auxiliary substances - nucleating, precipitating, and hydrolyzing agents. Hydroxide precipitates were washed from reagent residues, lyophilized at 105 °C, and treated by the thermal method at T 600 and 800 °C for 5 h. The content of cerium oxide in the composition of the synthesized samples varied from 60 to 100 mol.%, the content of lanthanum oxide reached up to 35 mol.%, and the content of dysprosium oxide did not exceed 20 mol.%. Only fluorite-type structures are formed under the following conditions according to the phase equilibrium diagram [26].

The phase composition of the samples was studied using powder X-ray phase analysis [29; 30]. The point of zero charge (PZC) of the particles was measured by potentiometric titration of their suspensions (1 wt.% of the dispersed phase) with the concentration of the dispersion medium NaCl 0.1, 0.01 mol/dm^3 with 0.1 M solutions of HCl and NaOH.

The study of the photocatalytic activity of nanoparticles obtained in the CeO_2-La_2O_3-Dy_2O_3 ternary systems was carried out during the decolorization of a Malachite green solution with a day concentration of 20 mg/dm^3 under the visible light action. To prepare the suspension 50 mg of the powder in the 50 ml of the dye solution was chosen. The sorption activity of the powder was evaluated by stirring the suspension in the dark for 30 min. To compare we performed the photocatalytical study under ultraviolet irradiation of the suspension at a wavelength of 254 nm. Measurements were performed after processing the suspension for 5, 15, 30, 45, 120, and 150 min. The removal of nanosized particles from the suspension was ensured by the action of a centrifugal field (8 g) for 20 min. The concentration was determined by measuring the optical density of the filtered solution using an Ulab 101 photo spectrometer at a wavelength of 540 nm by the constructed calibration graph. The degree of discoloration of the solution (D, %) was calculated according to the standard equation:

$$D, \% = (1-C/C_0)\cdot 100,$$

where C is the residual concentration of the dye, and C_0 is the initial concentration of the dye.

Experimental part

Structural characteristics of composite particles obtained in the CeO_2-La_2O_3-Dy_2O_3 system

According to X-ray phase analysis data, all obtained samples correspond to tetragonal syngonia and have the fluorite-type structure of Fm3m (PDF No. 02-1306). Fig. 1 show a typical diffractograms of a CeO_2 (80 mol.%)-La_2O_3 (10 mol.%)-Dy_2O_3 (10 mol.%) sample heat-treated at T = 600 °C (Fig. 1a), and at T = 800 °C (Fig. 1b).

Table 1 summarizes data on the parameter and volume of the unit cell, the size of the primary particles (CSR) and the value of the PZC of the samples obtained in CeO_2-La_2O_3 -Dy_2O_3 systems at the temperatures 600 and 800 °C.

The cationic radii of the REE that are included in the structure of the nanocomposites are the following [32]:

Dy^{3+} 90.8 pm < Ce^{4+} 92.1 pm < La^{3+} 101 pm

(pm = 10^{-12} m).

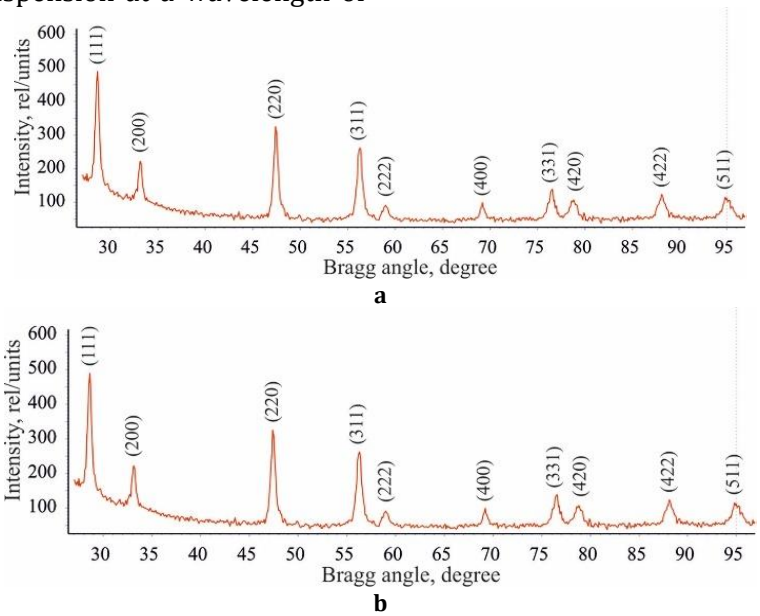

Fig. 1 XRD patterns of a samples with the chemical composition CeO_2 (80 mol.%) -La_2O_3 (10 mol.%) -Dy_2O_3 (10 mol.%) that were heat-treated for 5 h at the temperatures of °C: a – 600, b – 800.

Journal of Chemistry and Technologies, 2024, *32*(4), 887-894

Table 1

The crystal lattice parameters, primary particle's size, and PZC of the samples obtained in the CeO_2-La_2O_3-Dy_2O_3 systems

Composition, mol.%	Lattice parameter ***a***, nm	Volume of cell, nm^3	CSR, nm	PZC
	T = 600 °C, 5 h			
CeO_2(95)-Dy_2O_3(5)	0.5383	0.156	16.7	7.0
CeO_2(90)-La_2O_3(5)-Dy_2O_3(5)	0.5407	0.158	18.8	9.7
CeO_2(80)-La_2O_3(10)-Dy_2O_3(10)	0.5413	0.159	18.8	6.3
CeO_2(70)- La_2O_3(15)-Dy_2O_3(15)	0.5405	0.158	11.3	8.2
CeO_2(60)- La_2O_3(20)-Dy_2O_3(20)	0.5431	0.160	14.3	8.1
CeO_2(70)- La_2O_3(20)-Dy_2O_3(10)	0.5426	0.160	12.8	8.9
CeO_2(80)- La_2O_3(15)-Dy_2O_3(5)	0.5424	0.160	14.7	7.0
	T = 800 °C, 5 h			
CeO_2(95)-Dy_2O_3(5)	0.5381	0.156	26.5	8.5
CeO_2(90)- La_2O_3(5)-Dy_2O_3(5)	0.5406	0.158	20.1	-*
CeO_2(80)- La_2O_3(10)-Dy_2O_3(10)	0.5408	0.158	20.3	10.0
CeO_2(70)- La_2O_3(15)-Dy_2O_3(15)	0.5429	0.160	24.1	9.9
CeO_2(60)- La_2O_3(20)-Dy_2O_3(20)	0.5436	0.161	19.8	9.4
CeO_2(70)- La_2O_3(20)-Dy_2O_3(10)	0.5443	0.161	25.2	-
CeO_2(80)- La_2O_3(15)-Dy_2O_3(5)	0.5416	0.159	24.0	8.5

* - the measurement was not carried out

According to the obtained data, the primary particle's size (CSR) increases in the samples with an increase in the calcination temperature up to 800 °C. The unit cell parameter depends on the elemental composition of the samples: an increase in the mass content of lanthanum leads to an increase in the volume of the unit cell $V = a^3$.

Fig. 2 shows the SEM images of composite particles obtained in the ternary CeO_2-La_2O_3-Dy_2O_3 system at T = 600 °C. The particles are well crystallized and have a nanoscale size, averaging from 24 to 74 nm. The size of the aggregates reaches 250-300 nm.

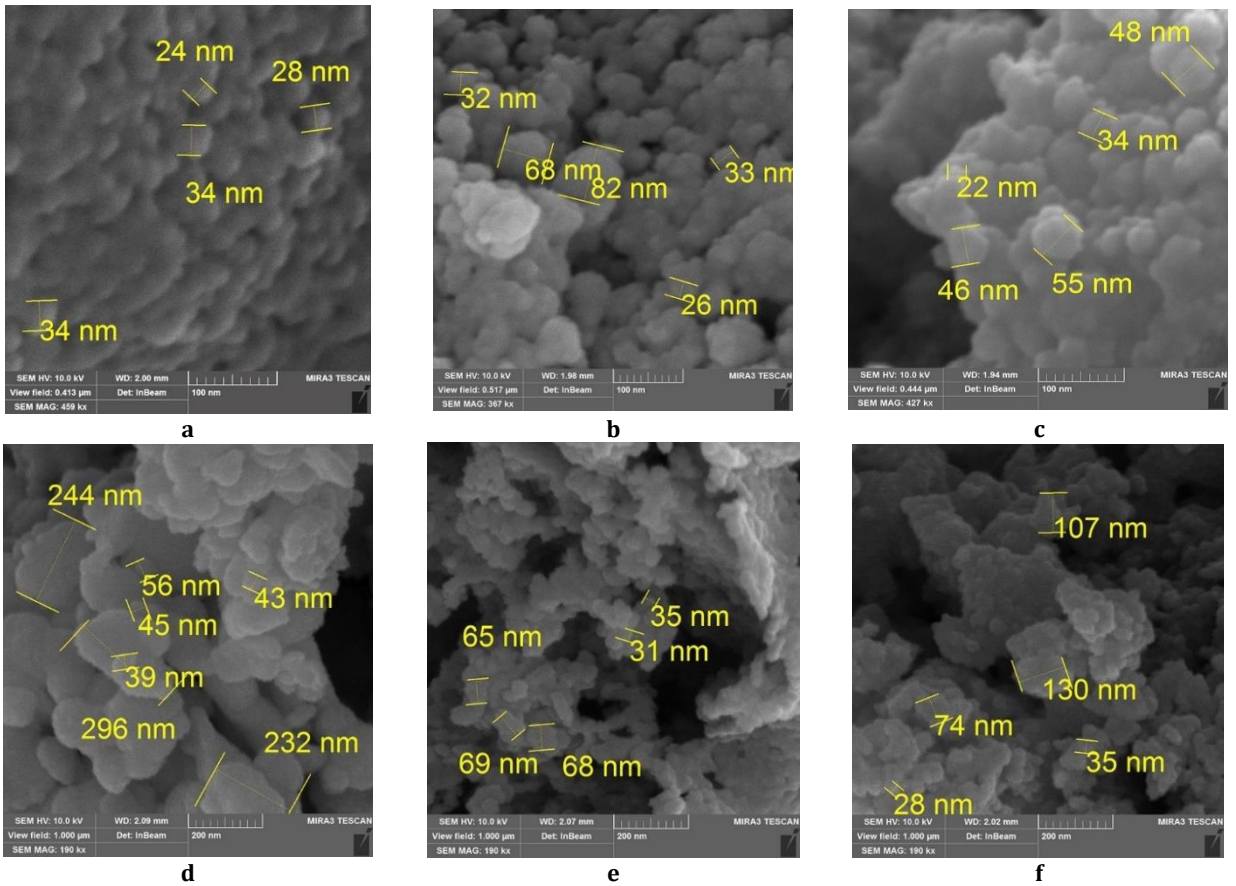

Fig. 2. SEM images of composite nanoparticles formed in CeO_2-La_2O_3-Dy_2O_3 systems (the mole percentage is given in parentheses): a – CeO_2(95)-Dy_2O_3(5); b – CeO_2(90)-La_2O_3(5)-Dy_2O_3(5); c – CeO_2(80)-La_2O_3(10)-Dy_2O_3(10); d – CeO_2(70)-La_2O_3(15)-Dy_2O_3(15); e – CeO_2(60)-La_2O_3(20)-Dy_2O_3(20); f – CeO_2(80)-La_2O_3(15)-Dy_2O_3(5).

Journal of Chemistry and Technologies, 2024, *32*(4), 887-894

Photocatalytic activity study of nanocomposites obtained in the CeO_2-La_2O_3-Dy_2O_3 systems

The comparison of the sorption and photocatalytic activity of particles under the visible light and UV, obtained in the ternary CeO_2-La_2O_3-Dy_2O_3 systems, are given in Tables 2–4. Cerium-based nanocomposite particles modified with lanthanum and dysprosium showed photocatalytic activity in the visible light region. The research was conducted in a neutral medium at pH=6.5. According to the data presented in Table 2 and Table 3, the increasing Dy_2O_3 and La_2O_3 concentrations from 10 mol.% to 20 mol.% does not affect the change in the photocatalytic activity of the composite. In both cases, after 30 min in the process of sorption-desorption, the concentration of the dye is identical and is 0.41 mg/dm^3, and the extraction of the dye reaches 98 %. After visible light action within 30–45 min, the data for the systems CeO_2 (80 mol.%)-La_2O_3 (10 mol.%)-Dy_2O_3 (10 mol.%) and CeO_2 (60 mol.%)-Dy_2O_3 (20 mol.%)-La_2O_3 (20 mol.%) also do not differ and the residual concentration of the dye is 0.45–0.46 mg/dm^3, and the extraction of the dye is ≈ 97.7–97.8 %.

Table 2

Photocatalytic activity of the particles obtained in the ternary CeO_2 (80 mol.%)-La_2O_3 (10 mol.%)-Dy_2O_3 (10 mol.%) system at 600 °C in 5 h

t, min	Sorption-desorption		t, min	Visible light		t, min	UV	
	C, mg/dm^3	R, %		C, mg/dm^3	R, %		C, mg/dm^3	R, %
7	0.68	96.6	60	0.45	97.8	5	0.92	95.4
15	0.53	97.4	90	0.34	98.3	10	0.88	95.6
25	0.41	97.9	120	0.34	98.3	20	0.85	95.8
35	0.41	98.0	24 h	0.07	99.7	30	0.81	95.9
60	0.35	98.3	-	-	-	40	0.77	96.2

* t – time of treatment, C- residual concentration of MG (Malachite green), R – degree of dye's destruction

Table 3

Photocatalytic activity of particles obtained in the binary CeO_2(95 mol.%)-Dy_2O_3 (5 mol.%) system at 600 °C in 5 h

t, min	Sorption-desorption		t, min	Visible light	
	C, mg/dm^3	R, %		C, mg/dm^3	R, %
5	0.85	95.8	30	0.67	96.7
10	0.78	96.1	60	0.41	97.9
20	0.63	96.9	24 h	0.44	97.8

* t – time of treatment, C- residual concentration of MG (Malachite green), R – degree of dye's destruction

Table 4

Photocatalytic activity of particles obtained in the ternary CeO_2 (80 mol.%)-La_2O_3 (10 mol.%)–Dy_2O_3 (10 mol.%) system at 800 °C in 5 h

t, min	Sorption-desorption		t, min	Visible light	
	C, mg/dm^3	R, %		C, mg/dm^3	R, %
5	0.87	95.7	45	1	95.0
15	0.89	95.6	60	0.83	95.9
20	1.09	94.6	120	0.74	96.3
30	1	95.0	180	0.61	97.0
-	-	-	24 h	0.32	98.4

* t – time of treatment, C- residual concentration of MG (Malachite green), R – degree of dye's destruction

Increasing the temperature of heat treatment of the studied samples CeO_2 (60 mol.%) – Dy_2O_3 (20 mol.%) – La_2O_3 (20 mol.%) to 800 °C reduces their photocatalytic activity (Table 5). The obtained results show, the residual concentration of the dye after 30 min of the sorption-desorption process is 0.41 mg/dm^3 for the sample preheated at 600 °C and 0.60 mg/dm^3 for the sample sintered at 800 °C. Accordingly, extraction of the dye from the solution is greater at T=600 °C (98 %), and less at T=800 °C (97 %).

Table 5

Journal of Chemistry and Technologies, 2024, *32*(4), 887-894

Photocatalytic activity of particles obtained in the ternary CeO_2(60 mol.%)-Dy_2O_3(20 mol.%)-La_2O_3(20 mol.%) systems at 600 and 800 °C

T=600 °C						T=800 °C					
t, min	Sorption-desorption		t, min	Visible light		t, min	Sorption-desorption		t, min	Visible light	
	C, mg/dm³	R, %		C, mg/dm³	R, %		C, mg/dm³	R, %		C, mg/dm³	R, %
5	0.37	98.1	45	0.41	98.0	10	0.65	96.8	15	0.46	97.7
10	0.52	97.4	60	0.30	98.5	30	0.60	97.0	30	0.46	97.7
20	0.52	97.4	90	0.44	97.4	60	0.52	97.4	24 h	0.25	98.8
30	0.41	98,0	120	0.37	98.2	-	-	-	-	-	-

* t – time of treatment, C - residual concentration of MG (Malachite green), R – degree of dye's destruction

Carrying out classical photocatalysis under UV irradiation does not supply a positive result. This is confirmed by the data presented in Table 2, which characterizes the photocatalytic activity of particles obtained in the ternary system CeO_2 (80 mol.%) – La_2O_3 (10 mol.%) – Dy_2O_3 (10 mol.%) and thermally treated at 600 °C. As can be seen from the data in this Table, the residual concentration of 0.8 mg/dm³ of the dye remains almost unchanged even after 40 min of irradiation, and the dye destruction remains close to 96 %. The reaction under visible light conditions for the same system shows significant differences and dynamics, namely, after the first 7 min the degree of dye destruction is 97.8 %. The residual concentration of MG solution equals 0.45 mg/dm³. As the duration of the experiment increases, the residual dye's concentration decreases only after 24 hours up to 0.07 mg/dm³, and dye destruction reaches 99.7 %.

The measurement of PZC particles (Table 1) shows that at pH < 7.0 the particles have a positive charge (up to 10 mV), which positively affects their interaction with molecules of the cationic dye (MG) at a solution pH of 6.5.

Conclusion

1. Nanocomposite particles with a fluorite-type structure were obtained by the chemical synthesis, the composition of which includes from 95 to 60 mol.% CeO_2, from 10 to 20 mol.% La_2O_3, from 5 to 20 mol.% Dy_2O_3. The parameter of the tetragonal crystal lattice increases with an increase in the mol.% content of lanthanum, which is associated with its larger ionic radius (101 pm) compared to the ionic radii of dysprosium (90.8 pm) and cerium (92.1 pm). The primary particle size ranged from 11.3 to 18.8 nm for samples treated at 600 °C and from 19.8 to 26.5 nm for samples treated at 800 °C. The point of zero charge of the particles varied within 6.3 (7.0)–10, which affects the interaction of positively charged particles with the MG.

2. Cerium-based nanocomposite particles modified with lanthanum and dysprosium showed photocatalytic activity in the visible light region. The best photocatalytic properties demonstrated the particles with a composition of CeO_2 (80 mol.%)-La_2O_3 (10 mol.%)-Dy_2O_3 (10 mol.%), previously subjected to heat treatment at T=600 °C for 5 h. It was experimentally found that increasing the temperature of the preliminary heat treatment of the studied samples reduces their photocatalytic activity.

3. The impact of ultraviolet irradiation does not lead to the course of photocatalysis. In the ternary system CeO_2–La_2O_3–Dy_2O_3 under the UV irradiation, the residual concentration of the dye practically does not change even after 40 min and is ≈ 0.8 mg/dm³, and the dye extraction remains at the level of 96 %, while the reaction under visible light conditions for that same system shows significant differences and dynamics.

References

[1] Zeng, S., Shui, A., Yu, H., He, C. (2024). Sonochemical synthesis of CeO_2 nanoparticles with high photocatalytic and antibacterial activities under visible light. *Applied Ceramic Technology*, 21, 3141–3151. https://doi.org/10.1111/ijac.14775

[2] Xu, Y., Zhou, Y., Li, Y., Liu, Y., Ding, Z. (2024). Advances in cerium dioxide nanomaterials: Synthesis, strategies, property modulation, and multifunctional applications. *Journal of Environmental Chemical Engineering,* 12(5), 113719. https://doi.org/10.1016/j.jece.2024.113719

[3] Momin, Naeemakhtar., Manjanna, J., D'Souza, L., Aruna, S.T., Sentil Kumar, S. (2022). Synthesis, structure and ionic conductivity of nanocrystalline $Ce_{1-x}La_xO_{2-\delta}$ as an electrolyte for intermediate temperature solid oxide fuel cells. *Journal of Alloys and Compounds,* 896, 163012. https://doi.org/10.1016/j.jallcom.2021.163012

[4] Li, C., Zheng, Y., Li, M., Fang, B., Lin, J., Ni, J., Wang, X., Lin, B., Jiang, L. (2022). Enhancement of ammonia synthesis activity on La_2O_3-supported Ru catalyst by addition of ceria. *International Journal of Hydrogen*

Energy, 47(55), 23240–23248. https://doi.org/10.1016/j.ijhydene.2022.05.133

[5] Zhang, Y., Yan, Z., Xiao, M., Zhang, C., Ruan, L., Zhang, Y., Zhong, Y., Yan, Y., Yu, Y., He, H. (2025). Catalytic performance of Pd catalyst supported on CeO_2 or ZrO_2 modified beta zeolite for methane oxidation. *Journal of Environmental Sciences,* 152, 248–261. https://doi.org/10.1016/j.jes.2024.05.005

[6] Chen, J. P., Patil, S., Seal, S., McGinnis, J. F. (2006). Rare earth nanoparticles prevent retinal degeneration induced by intracellular peroxides. *Nature Nanotechnology*, 1, 142–150. https://doi.org/10.1038/nnano.2006.91

[7] van Deelen, T.W., Hernández Mejía, C., de Jong, K.P. (2019). Control of metal-support interactions in heterogeneous catalysts to enhance activity and selectivity. *Nature Catalysis,* 2(11), 955–970. https://doi.org/10.1038/s41929-019-0364-x

[8] Joshi, A., Chand, P., Saini, S. (2023). Improved electrochemical performance of rare earth doped $Bi_{1-x}M_xPO_4$ (x=0, 0.15; M=La, Ce, Sm) Nanostructures as electrode material for energy storage applications. *Journal of Alloys and Compounds*, *935*(2), 168063. https://doi.org/10.1016/j.jallcom.2022.1680639.

[9] 9.Stamatelos, I., Scheepers, F., Pasel, J., Dinh, C.-T., Stolten, D. (2024). Ternary Zn-Ce-Ag catalysts for selective and stable electrochemical CO_2 reduction at large-scale. *Applied Catalysis B: Environment and Energy,* 353, 124062. https://doi.org/10.1016/j.apcatb.2024.124062

[10] Wu, Q., Fu, H., Dang, C., Yang, G., Cao, Y., Wang, H., Wang, H.-F., Yu, H. (2024). In-modified Ni-CeO_2 for reverse water-gas shift: Cooperation between oxygen vacancies and intermetallic compounds. *Chemical Engineering Science*, 299(5), 120547. https://doi.org/10.1016/j.ces.2024.120547

[11] Shukla, M.K., Balyan, Y., Kumar, A., Bhaskar, T., Dhar, A. (2022). Catalytic oxidation of soot by CeO2-ZrO2 catalysts: Role of Zr. *Materials Chemistry and Physics,* 286(1), 126161. https://doi.org/10.1016/j.matchemphys.2022.126161

[12] Wang, C., Huang, W., Wang, Y., Cheng, Y.L., Zou, B.L., Fan, X.Z., Yang G.L., Cao, X.Q. (2012). Synthesis of monodispersed $La_2Ce_2O_7$ nanocrystals via hydrothermal method: A study of crystal growth and sintering behavior. *International Journal of Refractory Metals and Hard Materials, 31*, 242–246. 10.1016/j.ijrmhm.2011.12.002

[13] Liying, H.E., Yumin, S.U., Lanhong, Jiang., Shikao, S.H.I. (2015). Recent advances of cerium oxide nanoparticles in synthesis, luminescence and biomedical studies: a review. *Journal of Rare Earths, 33*(8), 791–799. https://doi.org/10.1016/S1002-0721(14)60486-5

[14] Kandasamy, P., Kandala, B., Wook Lee, M., Sivakumar, G. (2024). Phase stability and initial phase high-temperature corrosion behavior of non-stoichiometric lanthanum cerium oxide thermal barrier coatings. *Ceramics International, 50*(9), 14458–14468. https://doi.org/10.1016/j.ceramint.2024.01.358

[15] Chen, K., Wan, J., Wang, T., Sun, Qi., Zhou, R. (2023). Construction of bimetallic Pt–Pd/CeO_2–ZrO_2–La_2O_3 catalysts with different Pt/Pd ratios and its structure–activity correlations for three-way catalytic performance. *Journal of Rare Earths,* 41(6), 896–904. https://doi.org/10.1016/j.jre.2022.10.014

[16] Seminko, V.V., Maksimchuk, P.O., Sedyh, O.O., Aslanov, A.V., Malyukin, Yu. V. (2020). Improving •OH scavenging properties of nanoceria by doping and pre-irradiation. *Functional Materials,* 27(1), 6–11. doi: 10.15047/fm27.01/06

[17] Zarur, A.J., Ying, J.Y. (2000). Reverse microemulsion synthesis of nanostructured complex oxides for catalytic combustion. *Nature*, 403, 65–67. https://doi.org/10.1038/47450

[18] Schicks, J., Neumann, D., Specht, U., Veser, G. (2003). Nanoengineered catalysts for high-temperature methane partial oxidation, *Catalysis Today, 81*(2), 287–296. https://doi.org/10.1016/S0920-5861(03)00116-0

[19] Coduri, M., Checchia, S., Longhi, M., Ceresoli, D., Scavini, M. (2018). Rare Earth Doped Ceria: The Complex Connection Between Structure and Properties. *Frontiers Chemistry*, 6, 526. doi:10.3389/fchem.2018.00526

[20] Zheng, Y., Zhou, M., Ge, L., Li, Sh., Chen, H., Guo, L. (2011). Effect of Dy on the properties of Sm-doped ceria electrolyte for IT-SOFCs. *Journal of Alloys and Compounds, 509*(4), 1244–1248. doi:10.1016/j.jallcom.2010.09.203

[21] Jagjeet, K., Deepika, Ch., Vikas, D., Ravi, Sh., Yogita, P., Suryanarayana, N. S. (2016). Photoluminescence Characteristics of Dysprosium Doped CeO_2 Phosphor for White Light Emission. *J. Display Technol*, 12, 506–512. https://opg.optica.org/jdt/abstract.cfm?URI=jdt-12-5-506

[22] Trovarelli, A., and Llorca, J. (2017). Ceria catalyst at the nanoscale: How do crystal shapes shape catalysis? *ACS Catal,* 7, 4716–4735. doi: 10.1021/acscatal.7b01246

[23] Salehi, Z., Zinatloo-Ajabshir, S., Salavati-Niasari, M. (2017). Dysprosium cerate nanostructures: facile synthesis, characterization, optical and photocatalytic properties. *Journal of Rare Earths*, *35*(8), 805–812. doi: 10.1016/S1002-0721(17)60980-3

[24] Zinatloo-Ajabshir, S., Salehi, Z., Salavati-Niasari, M. (2018). Green synthesis and characterization of $Dy_2Ce_2O_7$ nanostructures using Ananas comosus with high visible-light photocatalytic activity of organic contaminants. *Journal of Alloys and Compounds, 763*, 314–321. https://doi.org/10.1016/j.jallcom.2018.05.311

[25] Kornienko, O.A., Andrievskaya, O.R., Barshchevskaya, H. K. (2020). [Phase relations in the system ternary based on ceria, zirconia and ytterbia at 1500 °C]. *Journal of Chemistry and Technologies, 28*(2), 142–152. https://doi.org/10.15421/082015 (In Ukrainian)

[26] Korniienko, O.A., Yushkevich, S.V., Bykov, O.I., Samelyuk, A.V., Bataiev, Yu.M., Zamula M.V. (2022). Phase equilibrium in binary La_2O_3-Dy_2O_3 and ternary CeO_2-La_2O_3-Dy_2O_3 systems. *Journal of the European Ceramic Society*, 42(13), 5820–5830 https://doi.org/10.1016/j.jeurceramsoc.2022.06.045

[27] Yushkevych, S.V., Korniienko, O.A., Bykov, O.I., Subota, I.S. (2023). Isothermal section for the ternary CeO_2–La_2O_3–Dy_2O_3 system at 1100 °C. *Journal of Chemistry and Technologies*, *31*(2), 215–222. https://doi.org/10.15421/jchemtech.v31i2.275434

[28] Torun, H.Ö., Kırkgeçit, R., Dokan, F.K., Öztürk, E. (2021). Preparation of La-Dy-CeO_2 ternary compound: Examination of photocatalytic and photoluminescence properties. *Journal of Photochemistry and Photobiology A: Chemistry*, 418, 113338. https://doi.org/10.1016/j.jphotochem.2021.113338

[29] Lavrynenko, O.M., Pavlenko, O.Yu., Zahornyi, M.N., Korichev, S.F. Morphology, phase and chemical

composition of the nanostructures formed in the systems containing lanthanum, cerium, and silver. (2021). *Chemistry, Physics and Technology of Surface*, 12, 4, 382–392. doi: 10.15407/hftp12.04.382

[30] Zahornyi, M.M., Lavrynenko, O.M., Kolomys, O.F., Strelchuk, V.V., Tyschenko, N.I., Korniienko, O.A., Ievtushenko, A.I. (2023). Modern Photoactive Nanocomposites Based on TiO_2 and CeO_2. *Journal of Nano-And Electronic Physics, 15*(4), 04001. https://doi.org/10.21272/jnep.15(4).04001

[31] Lavrynenko, O.M., Zahornyi, M.M., Vember, V.V., Pavlenko, O.Yu., Lobunets, T.F., Kolomys, O.F., Povnitsa, O.Yu., Artiukh, L.O., Naumenko, K.S., Zahorodnia, S.D., Garmasheva, I.L. (2022). Nanocomposites based on cerium, lanthanum, and titanium oxides doped with silver for biomedical application. *Condens. Matter (MDPI)*, *7*(3), 45. https://doi.org/10.3390/condmat7030045

[32] "Atomic and Ionic Radius". Chemistry LibreTexts. (2013). https://chem.libretexts.org/Bookshelves/Physical_and_Theoretical_Chemistry_Textbook_Maps/Supplemental_Modules_(Physical_and_Theoretical_Chemistry)/Physical_Properties_of_Matter/Atomic_and_Molecular_Properties/Atomic_and_Ionic_Radius